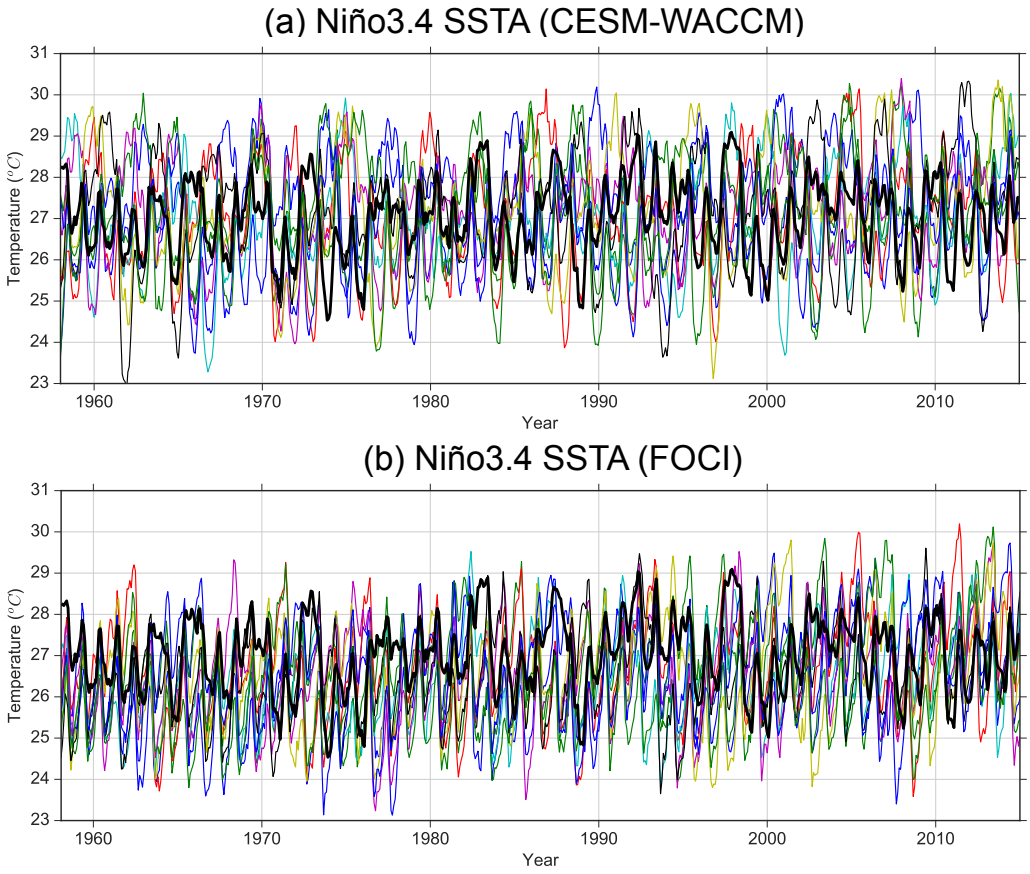

Figure S1: Comparison of individual ensemble members for CESM-WACCM (a), and FOCI (b) with reanalysis. The timeseries have not been detrended. The bold black line represents the ERSSTv5 from 1958 until 2014, while colored lines represent the different ensembles.

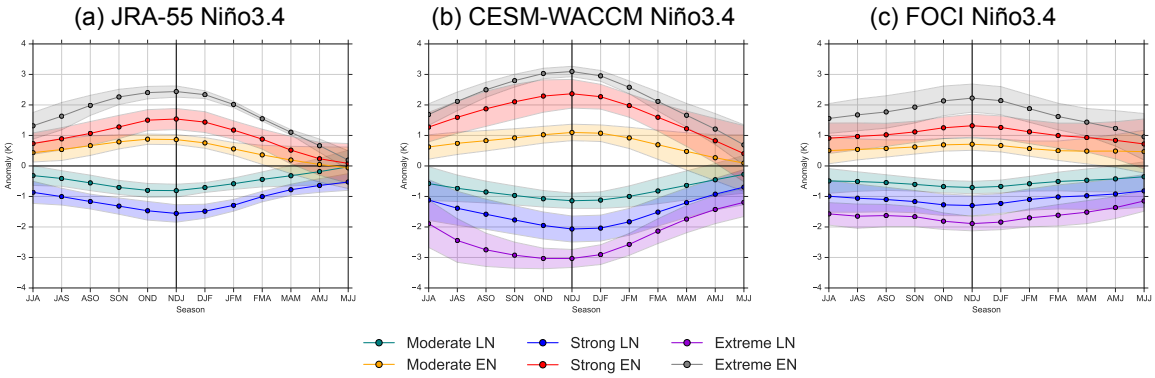

Figure S2: Composited 3-month average seasonal evolution of the Niño3.4 SSTA (in K) for JRA-55 (a, 1958-2021) and the ensemble means for CESM-WACCM (b), and FOCI (c). Events are subsampled into moderate, strong, and extreme events, as outlined in the methods. Shading represents the 95% confidence interval, while the solid line represents the mean.

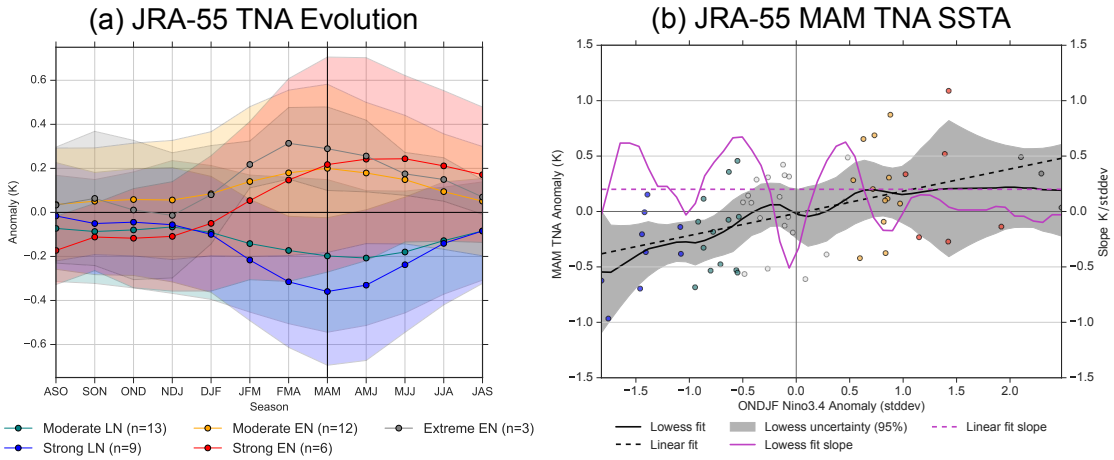

Figure S3: Composited 3-month seasonal evolution of the TNA SSTA (in K) (a) and the MAM TNA SSTA vs. the previous ONDJF Niño3.4 index (b) (see Figure 1a-b in manuscript for comparison). (b) shows the LOWESS curve in solid black, the 95% confidence interval for the LOWESS curve in shading, and the linear fit in the dashed line. The LOWESS curve is created using bootstrapping and resampling (with replacement) 1000 times. Methods follow Casselman et al. (2021).

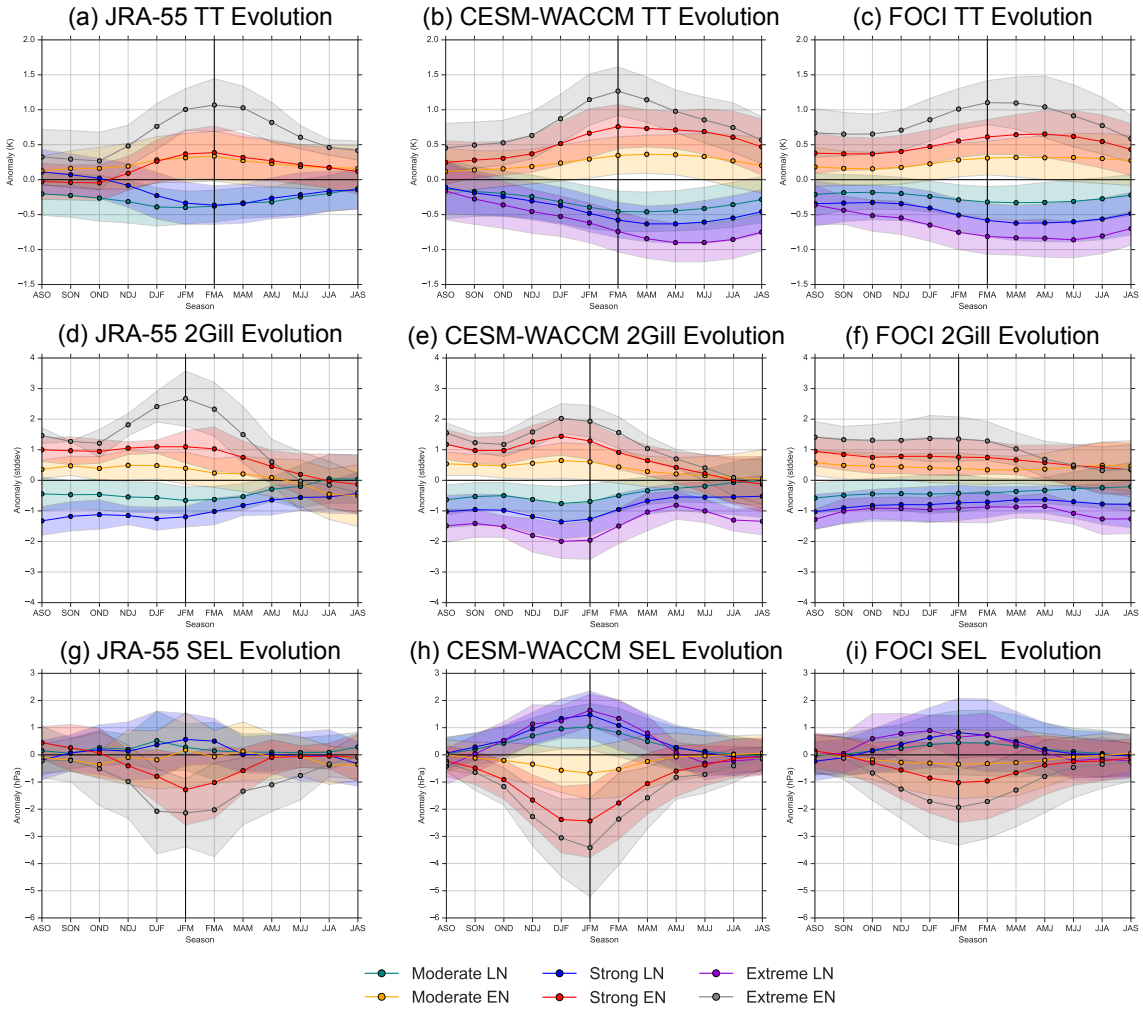

Figure S4: Similar to Supplementary Figure S2, except for the TT (top), Secondary Gill (2Gill, middle), and Southeastern Low (SEL, bottom) indices.

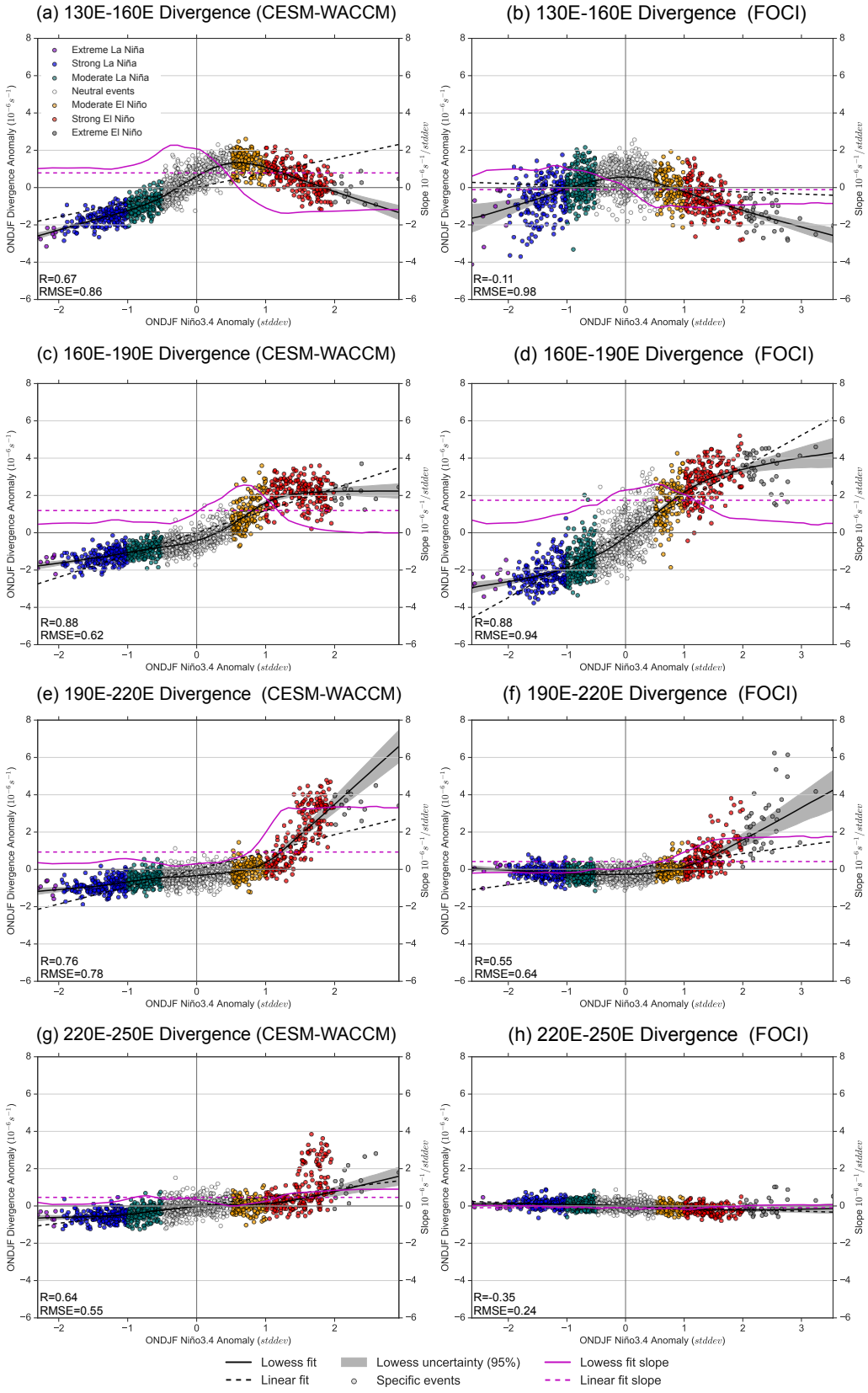

Figure S5: Relationship between the ONDJF Niño3.4 SSTA and ONDJF 200 hPa divergence over the Pacific. The divergence is averaged between 10°S-10°N, and varies between 130°E and 110°W (with 30° steps). Scatter plot coloring follows the same meaning as in Supplementary Figure S3.

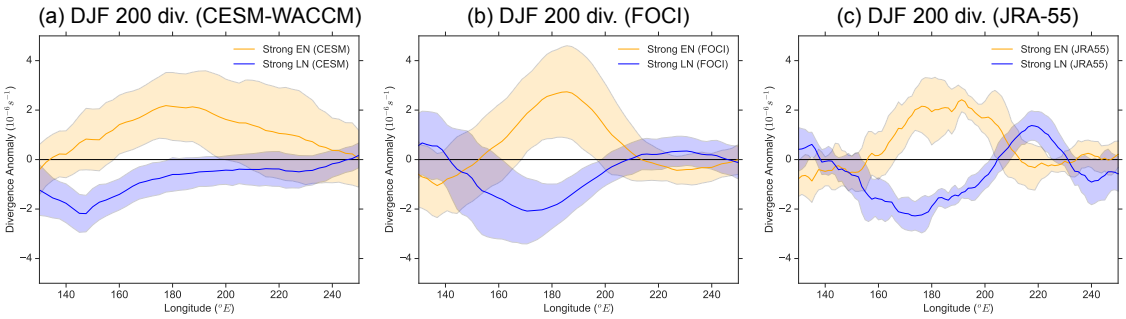

Figure S6: Divergence analysis over the tropical Pacific (averaged between 10°N-10°S) following an ENSO event. Panels a-c show the relationship between the ONDJF Niño3.4 SSTA and DJF 200 hPa divergence over the Pacific for CESM-WACCM (a), FOCI (b) and JRA-55 (c). Divergence is averaged between 10°S-10°N, and subsampled for strong events only (1-2 std dev), and shading represents ±1.0 std dev.

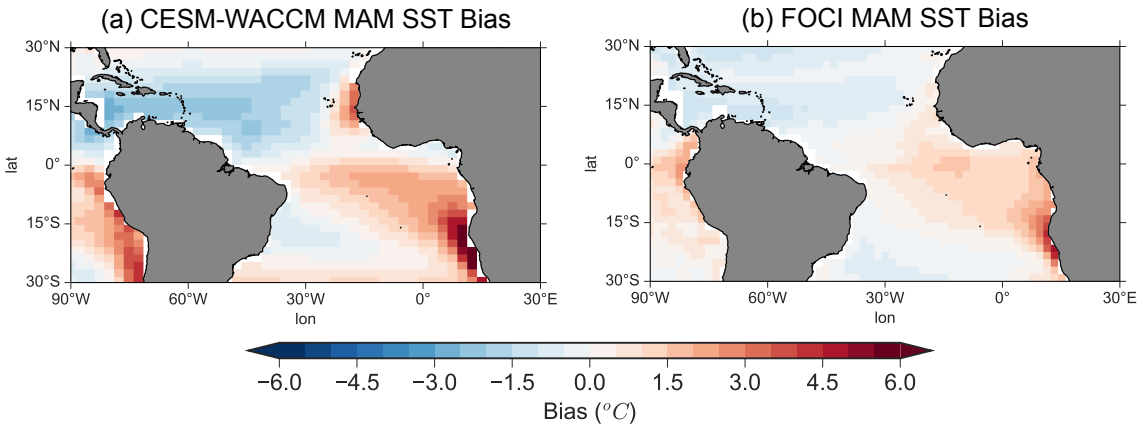

Figure S7: CESM-WACCM (left) and FOCI (right) SST bias with respect to ERSSTv5, with all datasets averaged from 1958 to 2014. ERSST is interpolated down to the grid of the given model, and the tropical (30°N-30°S) mean SSTs are removed from all datasets before computing the difference (model average minus ERSSTv5).

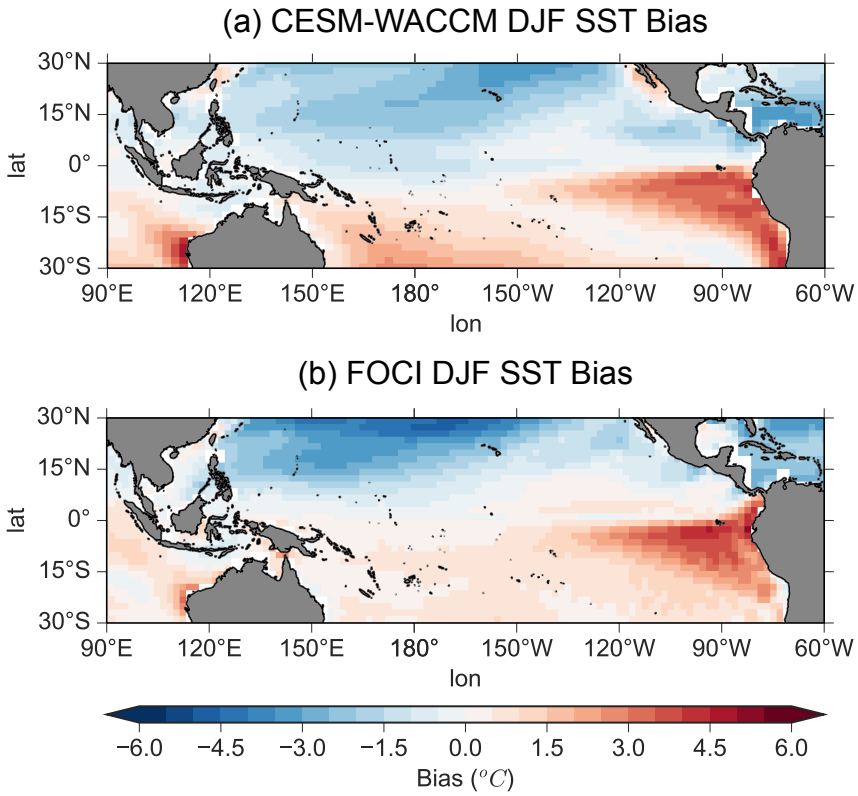

Figure S8: CESM-WACCM (left) and FOCI (right) SST bias with respect to ERSSTv5 using the same method as S7, except over the Pacific and averaged for December-February (DJF) instead.

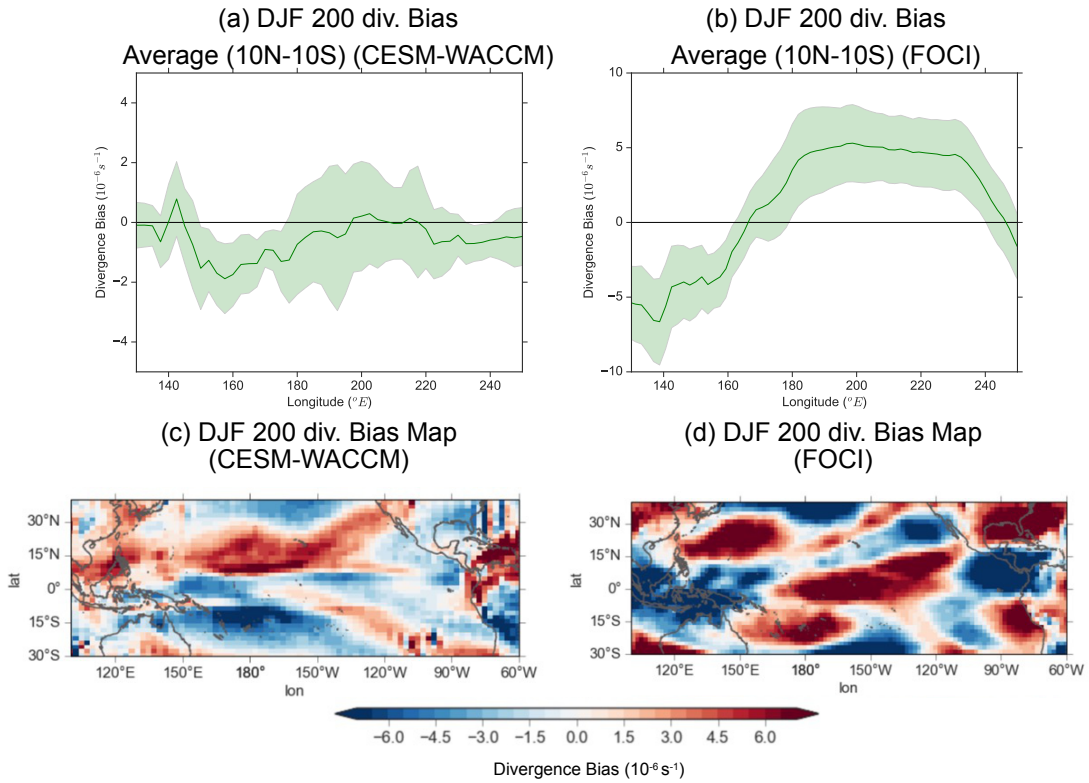

Figure S9: Divergence analysis over the tropical Pacific for background climatology biases. Panels a-b show DJF 200 hPa divergence bias averaged between 10°N-10°S with respect to JRA-55, while panels c-d show the mapped DJF 200 hPa divergence bias with respect to JRA-55. All datasets averaged between 1958 and 2014.

References

Casselman, J. W., A. S. Taschetto, and D. I. Domeisen, 2021: Non-linearity in the pathway of El Niño-Southern Oscillation to the tropical North Atlantic. *Journal of Climate*, 1–54, doi:10.1175/jcli-d-20-0952.1.